Since January 2020 Elsevier has created a COVID-19 resource centre with free information in English and Mandarin on the novel coronavirus COVID-19. The COVID-19 resource centre is hosted on Elsevier Connect, the company's public news and information website.

European Journal of Medicinal Chemistry 225 (2021) 113789

Contents lists available at ScienceDirect

European Journal of Medicinal Chemistry

journal homepage: http://www.elsevier.com/locate/ejmech

Discovery of juglone and its derivatives as potent SARS-CoV-2 main proteinase inhibitors

Jiahua Cui*, Jinping Jia*

School of Chemistry and Chemical Engineering, Shanghai Jiao Tong University, Shanghai, China

ARTICLE INFO

Article history:
Received 27 April 2021
Received in revised form
8 August 2021
Accepted 15 August 2021
Available online 18 August 2021

Keywords:
Naphthoquinones
Juglone
M^{pro} inhibitors
SARS-CoV-2
COVID-19

ABSTRACT

SARS-CoV-2 as a positive-sense single-stranded RNA coronavirus caused the global outbreak of COVID-19. The main protease (M^{pro}) of the virus as the major enzyme processing viral polyproteins contributed to the replication and transcription of SARS-CoV-2 in host cells, and has been characterized as an attractive target in drug discovery. Herein, a set of 1,4-naphthoquinones with juglone skeleton were prepared and evaluated for the inhibitory efficacy against SARS-CoV-2 M^{pro}. More than half of the tested naphthoquinones could effectively inhibit the target enzyme with an inhibition rate of more than 90% at the concentration of 10 μM. In the structure-activity relationships (SARs) analysis, the characteristics of substituents and their position on juglone core scaffold were recognized as key ingredients for enzyme inhibitory activity. The most active compound, 2-acetyl-8-methoxy-1,4-naphthoquinone (**15**), which exhibited much higher potency in enzyme inhibitions than shikonin as the positive control, displayed an IC_{50} value of 72.07 ± 4.84 nM towards M^{pro}-mediated hydrolysis of the fluorescently labeled peptide. It fit well into the active site cavity of the enzyme by forming hydrogen bonds with adjacent amino acid residues in molecular docking studies. The results from *in vitro* antiviral activity evaluation demonstrated that the most potent M^{pro} inhibitor could significantly suppress the replication of SARS-CoV-2 in Vero E6 cells within the low micromolar concentrations, with its EC_{50} value of about 4.55 μM. It was non-toxic towards the host Vero E6 cells under tested concentrations. The present research work implied that juglone skeleton could be a primary template for the development of potent M^{pro} inhibitors.

1. Introduction

Coronavirus disease 2019 (COVID-19) is a serious infectious disease caused by a new coronavirus named severe acute respiratory syndrome coronavirus 2 (SARS-CoV-2) [1,2]. The rapid spread of this pneumonia disease is an ongoing global threat that generates over 197 million diagnosed cases and more than 4.21 million deaths over 233 countries and territories globally by 03 Aug 2021 [3]. Until now, no clinically specific antiviral chemotherapeutics were available to treat the disease. The approved chemotherapeutic drugs against COVID-19 included favipiravir [4], lopinavir/ritonavir [5], chloroquine/hydroxychloroquine (FDA revoked emergency use authorization for chloroquine and hydroxychloroquine on June 15, 2020) [6], and remdesivir [7,8]. All of these drugs had been developed for the treatment of other related viruses, such as SARS and MERS coronavirus, Ebola, and HIV. Their degree of efficacy in COVID-19 treatment and the side effects were still controversial issues in academia [9–12]. The monoclonal antibody therapy employing bamlanivimab and antibody combination (bamlanivimab/etesevimab) has been authorized by FDA recently. However, certain variants of SARS-CoV-2 (B.1.351 and B.1.1.248) might escape from these neutralizing antibodies [13,14]. Therefore, it is urgent to explore targeted antiviral chemotherapeutics against SARS-CoV-2.

SARS-CoV-2 virus is a positive-sense single-stranded RNA virus [15,16], and its genome is translated to two overlapping polyproteins upon entry into host cells. The two polypeptides are proteolytically processed, mainly by a 33.8-kDa virus-specific main protease (M^{pro}), to afford proteins with different structures and functions required for replication [17,18]. The M^{pro} also referred to as the 3C-like protease modified the polyproteins at no less than 11 conserved amide linkages and played a pivotal role in the replication cycle of SARS-CoV-2 in host cells. Since closely related homologues of M^{pro} have never been identified in host cells, the protease is identified as a potential therapeutic target for the control of virus replication [19,20].

* Corresponding authors.
E-mail addresses: cpucjh@sjtu.edu.cn (J. Cui), jpjia@sjtu.edu.cn (J. Jia).

https://doi.org/10.1016/j.ejmech.2021.113789
0223-5234/

Natural products are a wellspring of lead compounds in drug discovery [21], and several phytochemicals have been investigated for their therapeutic potentials against SARS-CoV-2 [22,23]. Previous studies conducted by Jin et al. indicted that shikonin (Fig. 1, **1**), a natural naphthoquinone isolated from *Lithospermum erythrorhizon* Sieb. *et* Zucc., was a strong inhibitor of SARS-CoV-2 M^{pro} with its IC_{50} value of 15.75 ± 8.22 μM [18]. However, due to the Michael addition of shikonin naphthazarin nucleus as electrophiles [24,25] and bioreductive alkylation of its side chain with nucleophilic biomolecules such as glutathione, proteins or DNA [26], shikonin demonstrated significant cytotoxic effects at concentrations ranging from 100 μg/mL to 10 ng/mL *in vitro* [27]. The toxicity of shikonin prevented its further development as an antiviral drug candidate. Therefore, rational structural modifications were essential to overcome the defects in the structure of this hallmark molecule.

The research results from mechanistic investigations implied that the side chain and adjacent phenolic hydroxyl group on core structure of shikonin tautomer (Fig. S1, **Supplementary Information**) played pivotal roles in bioreductive alkylation and conjugate addition with bionucleophiles [26], which gave rise to the cytotoxicity of shikonin. Accordingly, we decided to modify shikonin skeleton through a scaffold simplification strategy to get juglone derivatives with a more appropriate scaffold in terms of improving cellular toxicity.

Juglone (**2**) is a naturally occurring 1,4-naphthoquione identified in *Juglandaceae* species, which bears a simplified shikonin core structure. It exhibited comparably low cytotoxicity against normal peripheral blood mononuclear cells with its IC_{50} value of more than 5 μg/mL [28]. It had been prescribed as a remedy for the treatment of a variety of skin diseases in the early 1900s [29]. The synthetic 2-methyl-1,4-naphthoquione (menadione, **3**) that served as a nutritional supplement in animal feeding was also much less toxic [30]. The results from earlier clinical investigations demonstrated that no toxic effects were observed in patients with hypoprothrombinemia receiving menadione doses from 1 to 200 mg [31]. All of the findings mentioned above supported our initial hypothesis that scaffold simplification and modification of shikonin naphthazarin nucleus would be reasonable approaches to reduce the cytotoxicity of shikonin as a natural SARS-CoV-2 M^{pro} inhibitor.

As a continuing investigation of biological activities of 1,4-naphthoquinones with shikonin as a lead, and in order to contribute to the drug discovery against COVID-19, the present study afforded the discovery of juglone and its derivative as potent M^{pro} inhibitors of SARS-CoV-2, which are promising antiviral drug candidates in future research and development.

2. Results

Chemistry. As shown in Scheme 1, the starting material for this synthesis of 1,4-naphthoquinone (**5**) was 1-naphthylamine (**4**). The oxidation of 1-naphthylamine (**4**) with hydrogen peroxide and subsequent column chromatography afforded 1,4-naphthoquinone **5**. Further Thiele-Winter acetoxylation of 1,4-naphthoquinone and subsequent hydrolysis of naphthalene-1,2,4-triyl triacetate (**6**) afforded 2-hydroxy-1,4-naphthoquione (**7**) in high yield [32]. 2-Methyl-1,4-naphthoquinone (vitamin K3, **3**) was obtained by the oxidation of 2-methylnaphthalene (**8**) using chromic anhydride in acidic conditions.

The reactions used to synthesize juglone (**2**) and its derivatives were outlined in Scheme 2. Juglone (**2**) was synthesized by the oxidation of 1,5-naphthelendiol (**9**) using the Fremy's salts, Soxhlet extraction, and further column chromatographic purification [33]. Juglone methyl ether (**10**) was obtained by the reductive methylation of juglone (**1**) with the presence of dimethyl sulfonate and sodium dithionate in alkali conditions and further cerium (IV) ammonium nitrate-mediated oxidative demethylation [34]. Propionyl juglone (**11**) and acetyl juglone (**12**) were prepared by the acylation of the parent compound by corresponding acid anhydride with sulfuric acid as the catalyst [35]. Acetyl juglone (**12**) was reduced by sodium dithionate to yield the hydroquinone intermediate. Migration of the acetyl group of hydroquinone in alkali conditions and further methylation afforded 4,8-dimethoxy-1-naphthol acetate (**13**) as the key intermediate [35]. Fries rearrangement of naphthol acetate (**13**) and subsequent CAN-mediated oxidation produced 2-acetyl-8-methoxy-1,4-naphthoquinone (**15**). 5,8-Dimethoxy-1,4-naphthoquinone (**21**) was prepared by the methylation of 1,5-naphthalenediol (**9**), subsequent bromination reactions, Cu(I)-catalyzed nucleophilic substitution [36], and further CAN-mediated oxidation (**Supplementary Information**).

7-Methyl juglone (**16**) and its derivatives (**22**–**25**) were prepared according to our reported procedures [37] resting on the Stobbe condensation of 2,5-dimethoxy benzaldehyde with diethyl succinate, intramolecular cyclization, reduction, acid-facilitated debenzylation and further oxidation. Plumbagin (**17**) was synthesized based on the reported procedure in which 1,5-naphthalenediol served as the starting point [38]. The substituted anthraquinone emodin (**18**), rhein (**19**) and aloe emodin (**20**) were prepared by the D-A reactions between diene and corresponding naphthoquinones [39,40].

Enzyme inhibition. Using a fluorescently labeled short peptide containing Q-S scissile bond, the inhibitory activity of the prepared quinones against M^{pro} of SARS-CoV-2 were evaluated according to the reported procedure [17]. Firstly, we tested the enzymatic inhibition rate of several naturally occurring naphthoquinones (juglone **2**, 7-methyl juglone **16**, lawsone **7**, plumbagin **17** and shikonin **1**), 9,10-anthraquinones (emodin **18**, rhein **19** and aloe emodin **20**) and the synthetic vitamin K3 (**3**) in the first library of compounds against SARS-CoV-2 M^{pro} at the concentration of 10 μM. The results from primary screening indicated that most of the natural quinones were ineffective, with the inhibition rate of less than 10% at 10 μM (Table S1, **Supplementary Information**). Vitamin K3 (**3**) with the inhibition rate of 12.7% was also inactive. The natural naphthoquinone shikonin, which had been identified as one of the

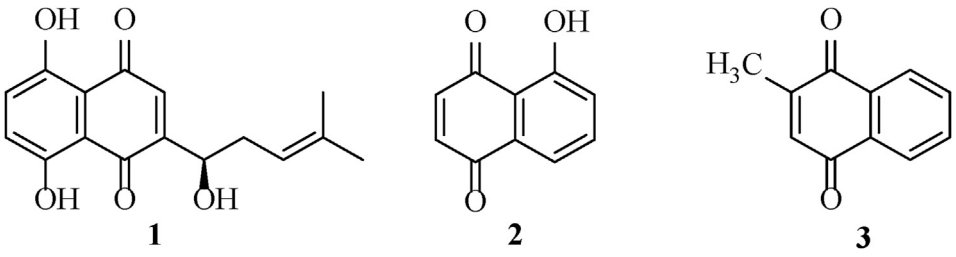

Fig. 1. The chemical structure of shikonin (**1**), juglone (**2**) and menadione (**3**).

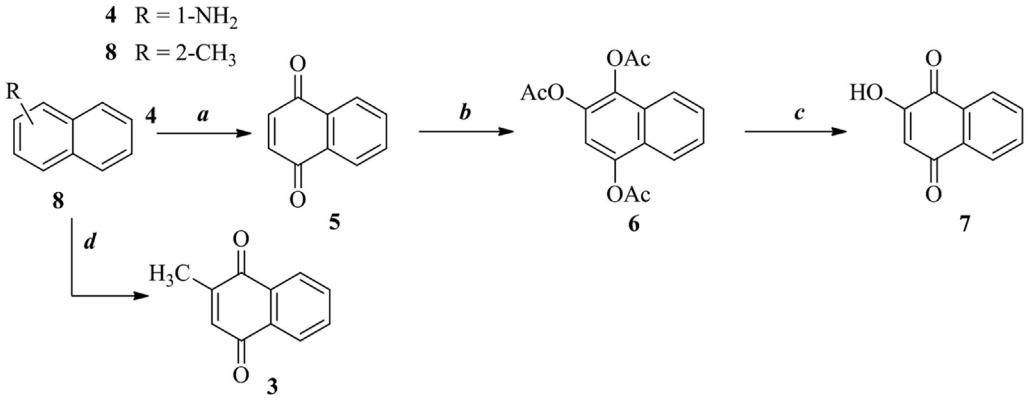

Scheme 1. Reagents and conditions: *a)* CH_3COOH, H_2SO_4, H_2O_2, 80 °C, 3 h; *b)* $(CH_3CO)_2O$, H_2SO_4, 10 °C, 8 h; *c)* CH_3ONa, CH_3OH, 5 °C; then conc. HCl; *d)* CrO_3, CH_3COOH, 40 °C for 30 min, then 65 °C for 20 min.

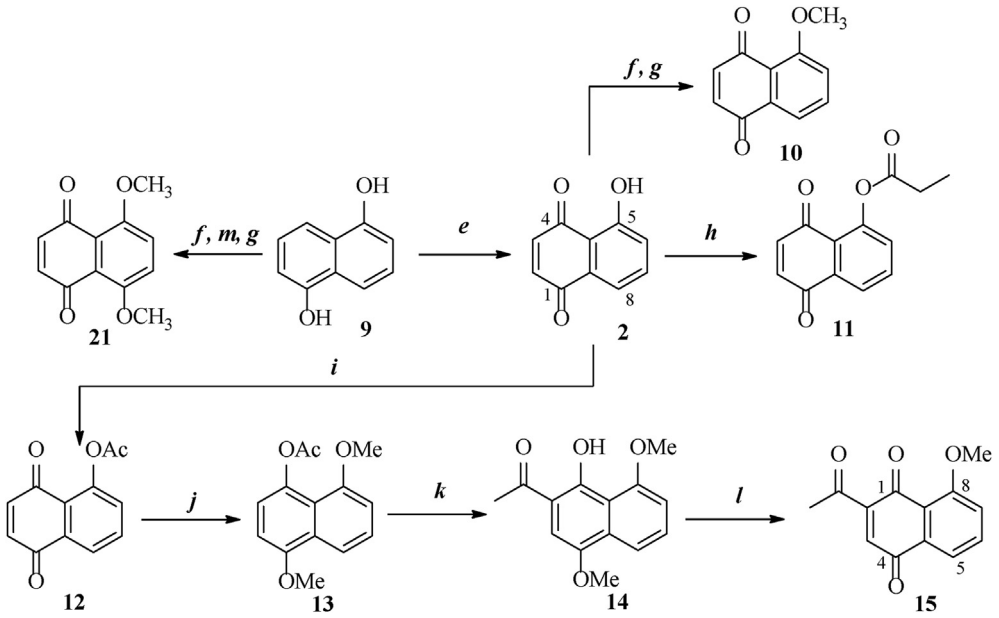

Scheme 2. Reagents and conditions: *e)* $(CH_3CO)_2O$, H_2O_2, 40–60 °C, 1 h; *f)* $(CH_3)_2SO_4$, NaOH, $Na_2S_2O_4$, Et_2O/H_2O, 5 °C, overnight; *g)* CAN, DCM-ACN (3:1), 5 °C; *h)* $(CH_3CH_2CO)_2O$, Cat. Conc. H_2SO_4, 5 °C, 4 h; *i)* $(CH_3CO)_2O$, Cat. Conc. H_2SO_4, 5 °C, 4 h; *j)* $Na_2S_2O_4$, Et_2O/H_2O, r.t., 2 h; then CH_3I, K_2CO_3, DMF, 10 °C, overnight; *k)* BF_3—Et_2O, 60 °C, 0.5 h; *l)* CAN, DCM-CAN (3:1), 5 °C, 0.5 h; *m)* NBS, ACN, −10 °C, overnight; then CH_3ONa, CuI, CH_3OH-DMF, reflux, 48 h.

strong M^{pro} inhibitors in previous studies (IC_{50} = 15.75 ± 8.22 μM) [17], was employed as the positive control. It demonstrated moderate inhibitory effects towards the target enzyme at the concentration of 10 μM. In the first library of naphthoquinones, juglone (**2**) and 7-methyl juglone (**16**) exhibited the strongest inhibition with the completely loss of the hydrolytic efficacy of M^{pro}. The two natural naphthoquinones were employed as the lead compounds for further structural modifications.

In the second library, the derivatives of juglone (**2**) and 7-methyl juglone (**16**) were produced by the addition of a few groups on their naphthoquinone scaffold and modifications on the phenolic hydroxyl group on the B-ring. The enzyme inhibition rate of compounds in the second library was displayed in Table S2. The results implied that almost all of the derivatives in the second library maintained the high inhibitory potency of juglone under concentrations of both 10 μM and 1 μM. At the concentration of 0.1 μM, a few analogues exhibited much higher potency as compared with the parent compounds (**2** and **16**). Then, the compounds with an enzymatic inhibition rate of more than 25% at the concentration of 0.1 μM entered the IC_{50} value screening (Table S3).

As shown in Table S3, within the tested synthetic 1,4-naphthoquinones as strong M^{pro} inhibitors, 2-acetyl-8-methoxy-1,4-naphthoquinone (**15**) was characterized as the most potent inhibitor against the target enzyme with its IC_{50} value of 72.07 ± 4.84 nM, which was comparable to the recently reported IC_{50} value of a short peptide as SARS-CoV-2 M^{pro} inhibitor (IC_{50} = 53 ± 5 nM) [17]. The 1,4-naphthoquinone (**5**) and propionyl juglone (**11**) have also been identified as potent inhibitors with IC_{50} value of 110.13 ± 7.04 and 129.77 ± 0.45 nM, respectively. 7-Methyl juglone ethyl acetate (**23**) and its benzyl ether (**25**) exhibited much higher IC_{50} values than propionyl juglone did.

Structure-activity relationship studies. In the first library of compounds (Table S1), the natural naphthoquinone juglone (**2**) exhibited potent inhibitory effects against the target SARS-CoV-2 M^{pro} with the inhibition rate of 99% at the concentration of 10 μM. By contrast, lawsone (**7**) as its analogue did not exhibit any detectable inhibition against M^{pro} under the same concentration. The sharp decrease in the activity should be ascribed to the

transposition of the B-ring hydroxyl group to the quinone ring. Compared with juglone, plambagin (**17**) with an additional methyl group on A-ring was also inactive towards M^{pro}. Similarly, the synthetic vitamin K3 (**3**) with a methyl group on the quinone ring displayed the enzymatic inhibition rate of only 12.7% as compared with the negative control. The elimination of the A-ring methyl group of vitamin K3 led to a significant increase in the efficacy in diminution of SARS-CoV-2 M^{pro} activity, because 1,4-naphthoquinone (**5**) as a strong inhibitor exhibited an IC_{50} value of only 110.13 ± 7.04 nM. The results demonstrated that both hydroxyl group and methyl substituent on the quinone ring had detrimental effects on the enzyme inhibitory potency of juglone (see Fig. 2).

7-Methyl juglone (**16**) with a methyl group on B-ring of juglone was as potent as compound **2** at 10 μM in the primary screening. At much lower concentrations, the enzyme inhibitory potency of 7-methyl juglone (inhibition rates of 99.6% and 21.7% at 1.0 μM and 0.1 μM, respectively) was slightly more potent than juglone. The results implied that the localization of a methyl group on C(2) of A-ring had deleterious effects while the exchange of the hydrogen atom on C(7) with a methyl group led to a slight increase in the activity. Furthermore, juglone and 7-methyl juglone were nearly two-fold more potent than shikonin as the control in inhibiting the target enzyme at the concentration of 10 μM. It was envisioned that the methyl substituent at C(7) on B-ring, instead of the corresponding six-carbon side chain of shikonin, could enhance the inhibitory potency.

The modifications of juglone on the chelated phenolic hydroxyl group have been shown to improve the inhibitory activity. Within the synthetic analogues, acetyl juglone and propionyl juglone showed higher potency than the parent compound juglone at the concentration of 1 μM. Methylation of the chelated phenolic hydroxyl group of juglone was not preferred because the corresponding methylated product (**10**) was less potent in enzymatic inhibition assay. The introduction of another methoxy group at C(8) on B-ring of juglone methyl ether (**10**) caused a further reduction in activity since the enzymatic inhibition rate of compound **21** was less than 80% at concentrations of 10 μM and 1.0 μM. Introduction of another acetyl substitution on C(2) adjacent to the C(1) carbonyl moiety led to increased activity, and compound **15** was identified as the most potent inhibitors among the prepared juglone derivatives. The strong electron withdrawing effects possibly contributed to the tight binding affinity of compound **15** with the target enzyme. The results implied that there might be some positive or negative interactions between the acetyl substituent on the quinone ring and the methyl group attached to the phenolic hydroxyl group of juglone.

The annulation of the quinone moiety with another phenyl group led to a drastic decrease in the enzymatic inhibition potency, because emodin (**18**), rhein (**19**) and aloe emodin (**20**) as derivatives of 7-methyl juglone showed the inhibition rate of less than 10%. The increased steric hindrance of the annulated phenyl ring caused detrimental effects on binding 7-methyl juglone with the target enzyme.

The methylation of 7-methyl juglone led to a drop in the activity at low concentrations, and 7-methyl juglone methyl ether (**22**) did not show any inhibitory effects towards the target enzyme at the concentration of 0.1 μM. Protection of the phenolic hydroxyl group with a methoxy methyl ether moiety also had deleterious effects since the M^{pro} inhibition rate of compound **24** was lower than 5% at concentrations of less than 1.0 μM. By contrast, both acylation and benzylation of the phenolic hydroxyl group of 7-methyl juglone caused an increase in potency at the concentration of 0.1 μM. The benzylated compound **25** exhibited an IC_{50} value of 160.68 ± 17.83 nM towards the target enzyme (Table S3), which was less than three-quarters of the value for the acylated derivative **23** (IC_{50} = 220.90 ± 14.03 nM).

Molecular docking. In order to gain an insight into the binding interaction of investigated naphthoquinones with SARS-CoV-2 M^{pro} enzyme, we performed molecular docking studies based on the crystal structures of M^{pro} in complex with the peptide-like inhibitor N3 (PDB ID: 6LU7). As shown in Fig. 3, both juglone (***a***), propionyl juglone (***b***) and 2-acetyl-8-methoxy-1,4-naphthoquinone (***c***) tightly fit the active site cavity of the enzyme. Juglone was bound to the target enzyme with the calculated binding energy of −8.6771 kJ/mol. The docking results indicated that the C(1) carbonyl group formed a hydrogen bond with Gly^{143} amino acid residue. Another hydrogen bonding interaction between the phenolic hydroxyl group and Glu^{166} was also observed.

The molecular docking study of propionyl juglone with the crystal structure of M^{pro} (**Fiure 3**, ***b***) showed that this ligand fit well into the substrate binding site of M^{pro} enzyme. Propionyl juglone was bound to the target enzyme with the calculated binding energy of −17.3199 kJ/mol, which was the lowest value for all of the predicted 30 binding models in MOE molecular docking. The oxygen atom of the C(4) carbonyl group underwent simultaneous H-bonding interactions with the backbone NH of Gly^{143} and the hydroxyl group of Ser^{144}.

2-Acetyl-8-methoxy-1,4-naphthoquinone (**15**) as the most

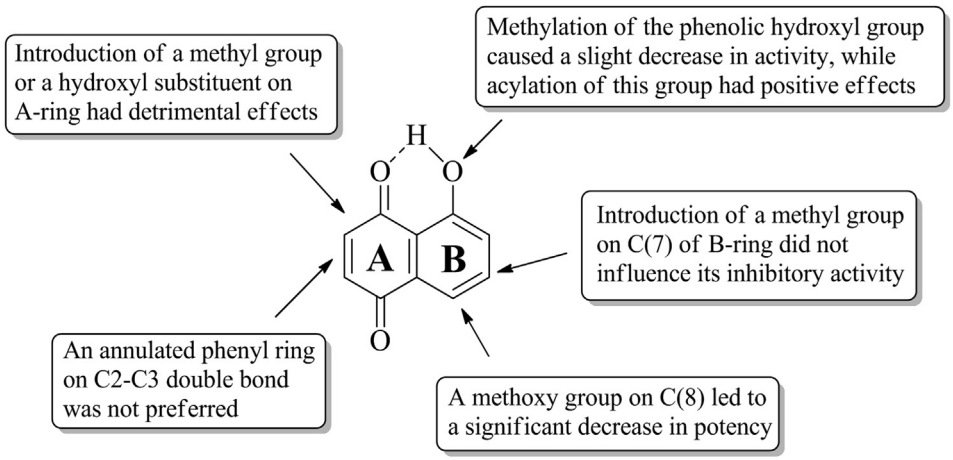

Fig. 2. SARs analysis of juglone and its derivatives as SARS-CoV-2 M^{pro} inhibitors.

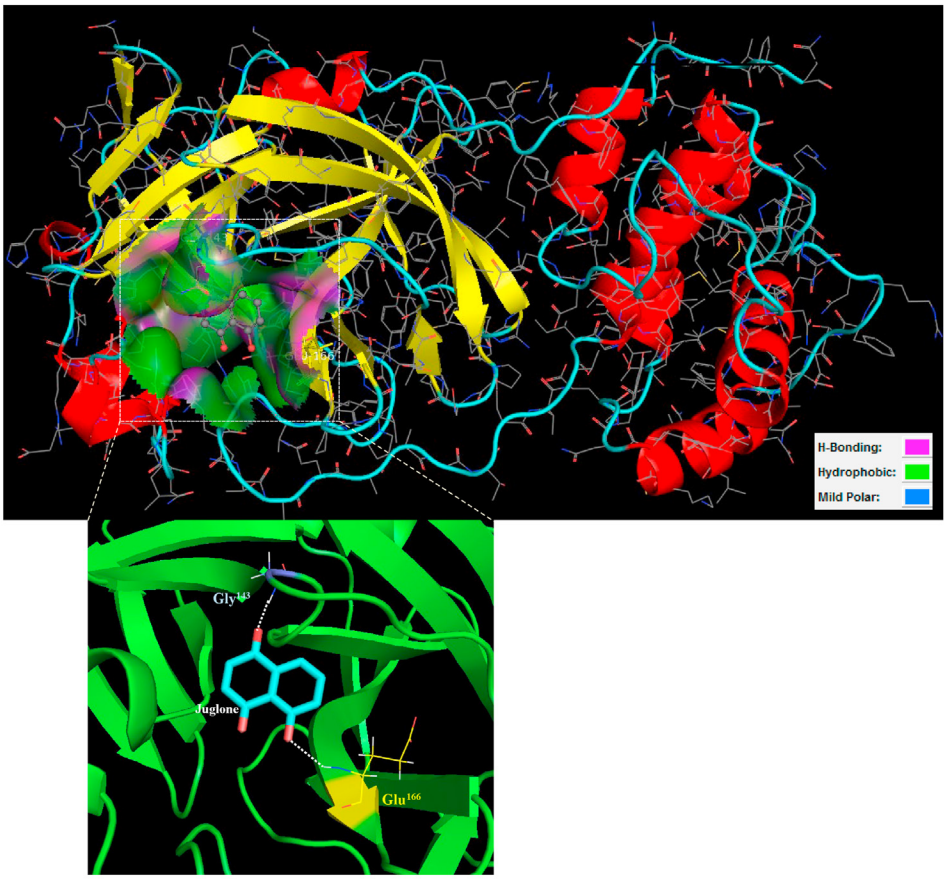
H-Bonding:
Hydrophobic:
Mild Polar:
Gly143
Juglone
Glu166

a

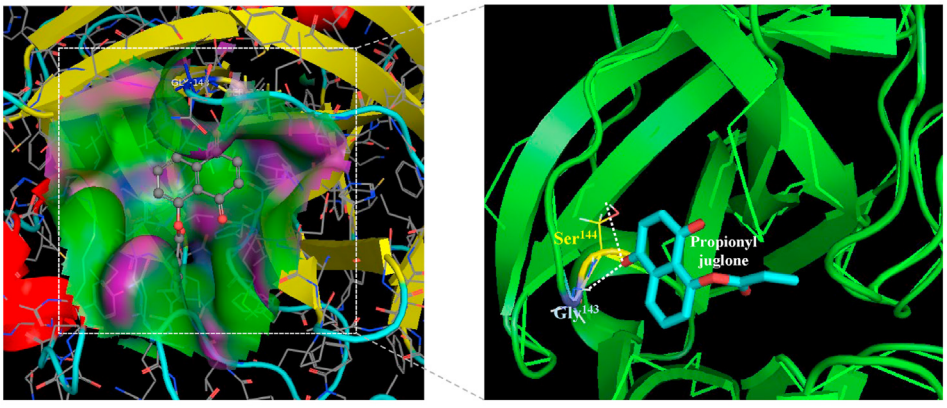
Ser144
Propionyl juglone
Gly143

b

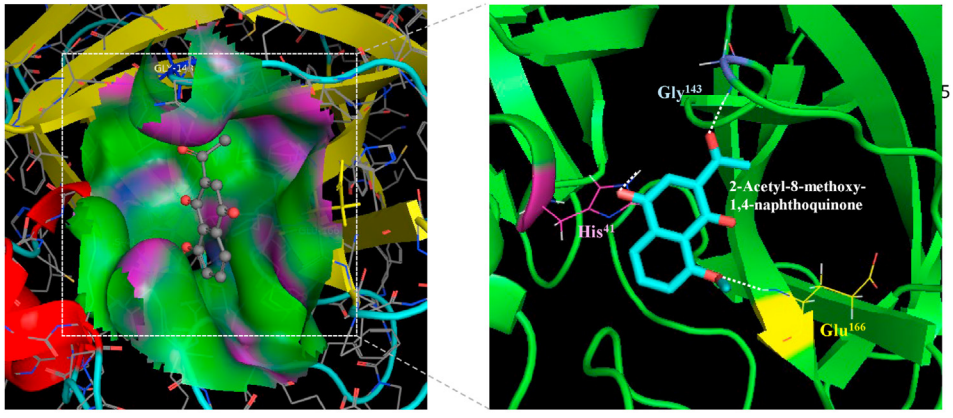
Gly143
2-Acetyl-8-methoxy-1,4-naphthoquinone
His41
Glu166

c

Fig. 3. The predicted binding modes of juglone (***a***), propionyl juglone (***b***) and 2-acetyl-8-methoxy-1,4-naphthoquinone (***c***) in the active site cavity of M^{pro}.

potent inhibitor against the target enzyme in the study was also bound to the substrate binding site of M^{pro} (Fig. 3, ***c***). The C(4) carbonyl group was oriented towards the imidazole moiety of His^{41} with the formation of a hydrogen bonding interaction. The oxygen atom on the acetyl substitution also hydrogen bonded with the backbone of NH of Gly^{143}. The methoxy group of compound **15** was placed towards Glu^{166}, and there was an H-bonding interaction between the oxygen atom in the methoxy group and NH in the amide backbone of Glu^{166}. The tight binding interaction between 2-acetyl-8-methoxy-1,4-naphthoquinone (**15**) and the target enzyme should explain its potent inhibitory activity against the enzymatic activity of M^{pro}.

Cytotoxicity of Juglone and its derivatives. The ideal antivirus agents were those ones that acted by inhibiting viral replication, but without cytotoxicity towards host normal cells [41]. Therefore, juglone and its derivatives as SARS-CoV-2 M^{pro} inhibitors were initially tested for their cytotoxic activity against human normal fibroblast HFF-1 cells using the standard MTT assay. As presented in Table S4, the naturally occurring juglone (**2**), 7-methyl juglone (**16**), and shikonin (**1**) exhibited potent growth inhibition towards the proliferation of HFF-1 cells with their IC_{50} values of less than 5 μM. The methylation and acylation of the phenolic hydroxyl group of juglone led to a minor decrease in cytotoxicity. Propionyl juglone (**11**) as a potent M^{pro} inhibitor was also toxic towards normal HFF-1 cells. It possibly underwent hydrolysis catalyzed by cytoplasmic enzymes to afford juglone (**2**) as a cytotoxic metabolite (Fig. 4). By contrast, the absence of the B-ring hydroxyl group of juglone caused a significant decrease in toxicity, because 1,4-naphthoquinone (**5**) exhibited a much higher IC_{50} value towards the normal HFF-1 cells.

The cytotoxicity of 7-methyl juglone (**16**) tended to be attenuated by the benzylation of the hydroxyl group on B-ring, and the IC_{50} value of compound **25** was 7-fold higher than that of the parent compound **16**. Lawsone (**7**) and vitamin K3 (**3**) with a substituent on the quinone ring displayed almost no cytotoxic effects on HFF-1 cells (IC_{50} > 50 μM). The electron donating effects and the steric hindrance of the group adjacent to the quinoidal carbonyl group prevented Michael addition of the quinone ring with nucleophilic biomolecules. 2-Acetyl-8-methoxy-1,4-naphthoquinone (**15**) was also much less toxic towards normal HFF-1 cells with its IC_{50} value of 41.2 μM. The presence of the acetyl moiety on A-ring prohibited the generation of ROS species and nucleophilic conjugate additions of quinone moiety with nucleophiles. Due to its strong inhibitory potency towards SARS-CoV-2 M^{pro} and low cytotoxic profile, it entered further *in vitro* antiviral activity evaluations.

Antiviral activity. The antiviral activity of compound **15** to inhibit SARS-CoV-2 replication *in vitro* was conducted according to the reported procedures [18]. 2-Acetyl-8-methoxy-1,4-naphthoquinone (**15**) exhibited antiviral activity at concentrations of more than 1 μM, with the half-maximal effective concentrations (EC_{50}) of 4.55 μM. The result indicated that the quinone (**15**) possibly penetrate cellular membranes and inhibit the target viral M^{pro} enzyme. The results from cytotoxicity evaluations implied that the compound was much less toxic than juglone towards normal HFF-1 cells. At the concentration of less than 20 μM, it didn't affect the growth of host Vero E6 cells (Fig. 5, ***b***, cell viability of more than 90%). Balb/C mice that received the preparation of the target compound (Fig. S2, 100 mg/kg, *p.o.*, on every the other day, 10 times

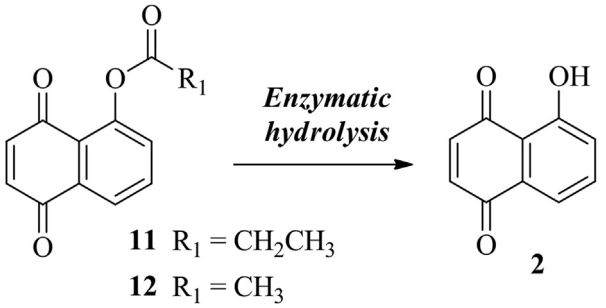

Fig. 4. The hydrolysis of propionyl juglone (**11**) and acetyl juglone (**12**).

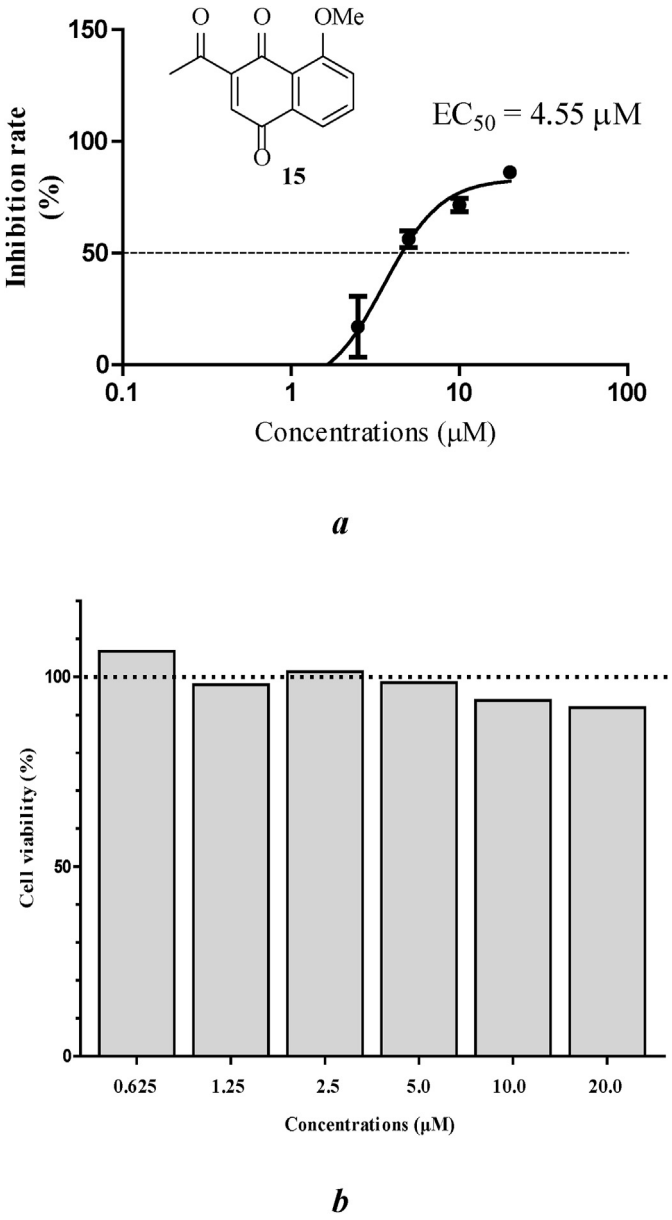

Fig. 5. *In vitro* inhibitory activity of compound **15** against SARS-CoV-2 in Vero E6. (***a***), the host Vero E6 cells were incubated with different concentrations of the target compound, and infected by SARS-CoV-2 *in vitro* with the MOI value of 0.05. The reproduced virus in cell culture was quantified by qRT-PCR assay. (***b***), the cell viability of host Vero E6 cells was determined by the standard MTT assay upon co-incubation of the cells with a series of concentrations of the indicated compound for 24 h.

in 20 days) did not show any obvious toxicity symptoms like reduced activity, hypothermia, or body shivering. Meanwhile, compound **15** induced no animal deaths and only caused a minor body weight loss as compared with control animals after a total treatment of 10 times in 20 days. As a potent M^{pro} inhibitor with antivirus activity, the juglone derivative **15** deserved further *in vivo* antiviral activity evaluation in future studies.

2.1. Discussion and future perspectives

Herein, we have described the discovery of juglone and its derivatives as potent M^{pro} inhibitors against SARS-CoV-2. Earlier chemical investigations disclosed the presence of juglone as a bioactive ingredient in *Exocarpium Juglandis Immaturum,* a traditional Chinese medicine used to treat psoriasis, ichthyosis, sores, and furuncles in the Orient [42]. It has also historically been used in European folk medicines as a remedy for parasites, ringworm, and other fungal infectious diseases [43]. The research results from previous investigations demonstrated that the natural naphthoquinone juglone was active against the animal *Vesicular Stomatitis* Virus [44] and it could potently reactivate latent HIV-1 in the bcl-2-transduced primary CD^{4+} T cell model [45].

The exact mechanism by which juglone acts against virus infections, however, still remains unclear. In our studies, this naphthoquinone was characterized as a potent inhibitor against SARS-CoV-2 M^{pro} by a high-throughput screening assay. It completely inactivated the main protease at the concentration of 1 μM. 3C-like proteases (M^{pro} in coronavirus), which belong to the cysteine protease family with a chymotrypsin-like fold, have been widely characterized in positive-sense single-stranded RNA viruses. In addition, 3C-like proteases shared several general similarities in substrate specificity and also inhibitor effectiveness [46]. Therefore, the structural features of juglone as a non-peptide inhibitor might act as a valuable scaffold for further anti-coronavirus drug design. Additionally, the results of our study also provided one explanation of the antiviral molecular mechanism of juglone.

Since the cleavage of viral proteins by specific proteases was crucial at post-entry stage in virus replication cycles, the SARS-CoV-2 M^{pro} was an attractive target for selective chemotherapeutic attack. The identified phytochemicals as M^{pro} inhibitors included glycosylated flavonoids [23,47], the diterpene andrographolide [48], the coumarin isopimpinellin [23], the naphthoquinone shikonin [18], and the alkaloid thalimonine [49]. However, most of these inhibitors were characterized in virtual screening. Data from *in vitro* evaluations were essential to confirm the potential of these phytochemicals in enzymatic inhibition.

In our studies, 2-acetyl-8-methoxy-1,4-naphthoquinone (**15**) exhibited the most potent inhibition against SARS-CoV-2 M^{pro} among the synthesized 1,4-naphthoquinones with its IC_{50} value in the nanomolar range. Compared with the naphthoquinone shikonin as a lead, it displayed more potent inhibitory effects against the target enzyme and showed much less cytotoxicity. The results from *in vitro* antiviral activity evaluation demonstrated that this inhibitor (**15**) effectively suppressed the replication of SARS-CoV-2 in Vero E6 cells with its EC_{50} value of 4.55 μM. All of these results supported that natural products and their derivatives are one of the most important sources of screening novel antiviral agents.

The data presented herein would be interpreted with emphasis, since the antiviral IC_{50} value of compound **15** may not reflect the results from actual *in vivo* experiments. Its antiviral efficacy against SARS-CoV-2 and safety should be further evaluated in adequate infected animal models. At present, the main impediment to the *in vivo* efficacy evaluation was the lack of generally applicable and validated animal models [50,51]. The recently established rhesus macaque model [52], which contributed to confirm the *in vivo* activity of remdesivir against SARS-CoV-2, might be used to test the treatment efficacy of other antiviral drug candidates in future. The *in vitro* research results confirmed by animal experiments would provide the rational basis for further research and development.

Author contributions

J. Cui and J. Jia conceived the idea. J. Cui performed the experiment and analyzed the data. J. Jia supervised the project. J. Cui and J. Jia wrote the paper.

Funding

This program was financially supported by Medical and Engineering Interdisciplinary Research Fund of Shanghai Jiao Tong University (Grant No. 20X190020002).

Declaration of competing interest

The authors declare that they have no known competing financial interests or personal relationships that could have appeared to influence the work reported in this paper.

Acknowledgement

We want to express our gratitude to Prof. Hong Liu and Prof. Yechun Xu in Shanghai Institute of Materia Medica, Chinese Academy of Sciences, for their valuable suggestions and also kind help in the biological evaluation. We also want to express our great appreciation to Prof. Gang Chen in School of Chemistry and Chemical Engineering, Shanghai Jiao Tong University, for the professional proof editing of our manuscript.

Appendix A. Supplementary data

Supplementary data to this article can be found online at https://doi.org/10.1016/j.ejmech.2021.113789.

References

[1] N. Zhu, D. Zhang, W. Wang, X. Li, B. Yang, J. Song, X. Zhao, B. Huang, W. Shi, R. Lu, P. Niu, F. Zhan, X. Ma, D. Wang, W. Xu, G. Wu, G.F. Gao, W. Tan, A novel coronavirus from patients with pneumonia in China, 2019, N. Engl. J. Med. 382 (2020) 727–733.

[2] J.A. Müller, R. Groß, C. Conzelmann, J. Krüger, U. Merle, J. Steinhart, T. Weil, L. Koepke, C.P. Bozzo, C. Read, G. Fois, T. Eiseler, J. Gehrmann, J. van Vuuren, I.M. Wessbecher, M. Frick, I.G. Costa, M. Breunig, B. Grüner, L. Peters, M. Schuster, S. Liebau, T. Seufferlein, S. Stenger, A. Stenzinger, P.E. MacDonald, F. Kirchhoff, K.M.J. Sparrer, P. Walther, H. Lickert, T.F.E. Barth, M. Wagner, J. Münch, S. Heller, A. Kleger, SARS-CoV-2 infects and replicates in cells of the human endocrine and exocrine pancreas, Nat. Metab. 3 (2021) 149–165.

[3] World Health Organization, Coronavirus Disease (COVID-19) Weekly Epidemiological Update and Weekly Operational Update, 2021. https://www.who.int/emergencies/diseases/novel-coronavirus-2019/situation-reports.

[4] V. Pilkington, T. Pepperrell, A. Hill, A review of the safety of favipiravir–a potential treatment in the COVID-19 pandemic? J. Virus Erad. 6 (2020) 45–51.

[5] H. Stower, Lopinavir–ritonavir in severe COVID-19, Nat. Med. 26 (2020) 465, 465.

[6] Z. Kashour, M. Riaz, M.A. Garbati, O. AlDosary, H. Tlayjeh, D. Gerberi, M.H. Murad, M.R. Sohail, T. Kashour, I.M. Tleyjeh, Efficacy of chloroquine or hydroxychloroquine in COVID-19 patients: a systematic review and meta-analysis, J. Antimicrob. Chemother. 76 (2021) 30–42.

[7] J.H. Beigel, K.M. Tomashek, L.E. Dodd, A.K. Mehta, B.S. Zingman, A.C. Kalil, E. Hohmann, H.Y. Chu, A. Luetkemeyer, S. Kline, D. Lopez de Castilla, R.W. Finberg, K. Dierberg, V. Tapson, L. Hsieh, T.F. Patterson, R. Paredes, D.A. Sweeney, W.R. Short, G. Touloumi, D.C. Lye, N. Ohmagari, M.-d. Oh, G.M. Ruiz-Palacios, T. Benfield, G. Fätkenheuer, M.G. Kortepeter, R.L. Atmar, C.B. Creech, J. Lundgren, A.G. Babiker, S. Pett, J.D. Neaton, T.H. Burgess, T. Bonnett, M. Green, M. Makowski, A. Osinusi, S. Nayak, H.C. Lane, Remdesivir for the treatment of covid-19 — final report, N. Engl. J. Med. 383 (2020) 1813–1826.

[8] Emergency Use Authorization. https://www.fda.gov/emergency-

preparedness-and-response/mcm-legal-regulatory-and-policy-framework/emergency-use-authorization, 2021.
[9] M. Guastalegname, A. Vallone, Could chloroquine/hydroxychloroquine be harmful in coronavirus disease 2019 (COVID-19) treatment? Clin. Infect. Dis. 71 (2020) 888–889.
[10] I. Torjesen, Covid-19: hydroxychloroquine does not benefit hospitalised patients, UK trial finds, BMJ 369 (2020) m2263.
[11] Y. Wang, D. Zhang, G. Du, R. Du, J. Zhao, Y. Jin, S. Fu, L. Gao, Z. Cheng, Q. Lu, Y. Hu, G. Luo, K. Wang, Y. Lu, H. Li, S. Wang, S. Ruan, C. Yang, C. Mei, Y. Wang, D. Ding, F. Wu, X. Tang, X. Ye, Y. Ye, B. Liu, J. Yang, W. Yin, A. Wang, G. Fan, F. Zhou, Z. Liu, X. Gu, J. Xu, L. Shang, Y. Zhang, L. Cao, T. Guo, Y. Wan, H. Qin, Y. Jiang, T. Jaki, F.G. Hayden, P.W. Horby, B. Cao, C. Wang, Remdesivir in adults with severe COVID-19: a randomised, double-blind, placebo-controlled, multicentre trial, Lancet 395 (2020) 1569–1578.
[12] Z. Khan, Y. Karataş, H. Rahman, Anti COVID-19 drugs: need for more clinical evidence and global action, Adv. Ther. 37 (2020) 2575–2579.
[13] M. Hoffmann, P. Arora, R. Groß, A. Seidel, B.F. Hörnich, A.S. Hahn, N. Krüger, L. Graichen, H. Hofmann-Winkler, A. Kempf, M.S. Winkler, S. Schulz, H.-M. Jäck, B. Jahrsdörfer, H. Schrezenmeier, M. Müller, A. Kleger, J. Münch, S. Pöhlmann, SARS-CoV-2 variants B.1.351 and P.1 escape from neutralizing antibodies, Cell 184 (2021) 2384–2393.
[14] M. Widera, A. Wilhelm, S. Hoehl, C. Pallas, N. Kohmer, T. Wolf, H.F. Rabenau, V.M. Corman, C. Drosten, M.J.G.T. Vehreschild, Bamlanivimab Does Not Neutralize Two SARS-CoV-2 Variants Carrying E484K in Vitro, medRxiv, 2021, https://doi.org/10.1101/2021.1102.1124.21252372.
[15] N. Schmidt, C.A. Lareau, H. Keshishian, S. Ganskih, C. Schneider, T. Hennig, R. Melanson, S. Werner, Y. Wei, M. Zimmer, J. Ade, L. Kirschner, S. Zielinski, L. Dölken, E.S. Lander, N. Caliskan, U. Fischer, J. Vogel, S.A. Carr, J. Bodem, M. Munschauer, The SARS-CoV-2 RNA–protein interactome in infected human cells, Nat. Microbiol. 6 (2021) 339–353.
[16] P. Zhou, X.-L. Yang, X.-G. Wang, B. Hu, L. Zhang, W. Zhang, H.-R. Si, Y. Zhu, B. Li, C.-L. Huang, H.-D. Chen, J. Chen, Y. Luo, H. Guo, R.-D. Jiang, M.-Q. Liu, Y. Chen, X.-R. Shen, X. Wang, X.-S. Zheng, K. Zhao, Q.-J. Chen, F. Deng, L.-L. Liu, B. Yan, F.-X. Zhan, Y.-Y. Wang, G.-F. Xiao, Z.-L. Shi, A pneumonia outbreak associated with a new coronavirus of probable bat origin, Nature 579 (2020) 270–273.
[17] W. Dai, B. Zhang, X.-M. Jiang, H. Su, J. Li, Y. Zhao, X. Xie, Z. Jin, J. Peng, F. Liu, C. Li, Y. Li, F. Bai, H. Wang, X. Cheng, X. Cen, S. Hu, X. Yang, J. Wang, X. Liu, G. Xiao, H. Jiang, Z. Rao, L.-K. Zhang, Y. Xu, H. Yang, H. Liu, Structure-based design of antiviral drug candidates targeting the SARS-CoV-2 main protease, Science 368 (2020) 1331–1335.
[18] Z. Jin, X. Du, Y. Xu, Y. Deng, M. Liu, Y. Zhao, B. Zhang, X. Li, L. Zhang, C. Peng, Y. Duan, J. Yu, L. Wang, K. Yang, F. Liu, R. Jiang, X. Yang, T. You, X. Liu, X. Yang, F. Bai, H. Liu, X. Liu, L.W. Guddat, W. Xu, G. Xiao, C. Qin, Z. Shi, H. Jiang, Z. Rao, H. Yang, Structure of Mpro from SARS-CoV-2 and discovery of its inhibitors, Nature 582 (2020) 289–293.
[19] L. Zhang, D. Lin, X. Sun, U. Curth, C. Drosten, L. Sauerhering, S. Becker, K. Rox, R. Hilgenfeld, Crystal structure of SARS-CoV-2 main protease provides a basis for design of improved α-ketoamide inhibitors, Science 368 (2020) 409–412.
[20] K. Steuten, H. Kim, J.C. Widen, B.M. Babin, O. Onguka, S. Lovell, O. Bolgi, B. Cerikan, C.J. Neufeldt, M. Cortese, R.K. Muir, J.M. Bennett, R. Geiss-Friedlander, C. Peters, R. Bartenschlager, M. Bogyo, Challenges for targeting SARS-CoV-2 proteases as a therapeutic strategy for COVID-19, ACS Infect. Dis. 7 (2021) 1457–1468.
[21] J. Cui, J. Jia, Natural COX-2 inhibitors as promising anti-inflammatory agents: an update, Curr. Med. Chem. 28 (2021) 3622–3646.
[22] S. Verma, D. Twilley, T. Esmear, C.B. Oosthuizen, A.-M. Reid, M. Nel, N. Lall, Anti-SARS-CoV natural products with the potential to inhibit SARS-CoV-2 (COVID-19), Front. Pharmacol. 11 (2020) 1514.
[23] A.M. Sayed, A.R. Khattab, A.M. AboulMagd, H.M. Hassan, M.E. Rateb, H. Zaid, U.R. Abdelmohsen, Nature as a treasure trove of potential anti-SARS-CoV drug leads: a structural/mechanistic rationale, RSC Adv. 10 (2020) 19790–19802.
[24] M.G. Miller, A. Rodgers, G.M. CoHen, Mechanisms of toxicity of naphthoquinones to isolated hepatocytes, Biochem. Pharmacol. 35 (1986) 1177–1184.
[25] V.P. Papageorgiou, A.N. Assimopoulou, E.A. Couladouros, D. Hepworth, K.C. Nicolaou, The chemistry and biology of alkannin, shikonin, and related naphthazarin natural products, Angew. Chem. Int. Ed. 38 (1999) 270–301.
[26] H.W. Moore, Bioactivation as a model for drug design bioreductive alkylation, Science 197 (1977) 527–532.
[27] H. Wagner, B. Kreher, K. Jurcic, In vitro stimulation of human granulocytes and lymphocytes by pico-and femtogram quantities of cytostatic agents, Arzneim. Forsch. 38 (1988) 273–275.
[28] R.C. Montenegro, A.J. Araújo, M.T. Molina, J.D.B.M. Filho, D.D. Rocha, E. Lopéz-Montero, M.O.F. Goulart, E.S. Bento, A.P.N.N. Alves, C. Pessoa, M.O. de Moraes, L.V. Costa-Lotufo, Cytotoxic activity of naphthoquinones with special emphasis on juglone and its 5-O-methyl derivative, Chem. Biol. Interact. 184 (2010) 439–448.
[29] C.J. Soderquist, Juglone and allelopathy, J. Chem. Educ. 50 (1973) 782–783.
[30] S. Ansbacher, W.C. Corwin, B.G.H. Thomas, Toxicity of menadione, menadiol and esters, J. Pharmacol. Exp. Therapeut. 75 (1942) 111–124.
[31] J.M. Macfie, A.L. Bacharach, M.R.A. Chance, A vitamin K analogue in obstructive jaundice, Br. Med. J. 2 (1939) 1220–1223.
[32] L.F. Fieser, Naphthoquinone antimalarials. III. Diene synthesis of 1, 4-naphthoquinones, J. Am. Chem. Soc. 70 (1948) 3165–3174.
[33] J. Cui, S. Li, An efficient synthesis of 5,6-dimethoxy 1- and 2-naphthols via Teuber reaction, J. Chin. Chem. Soc. 60 (2013) 1163–1168.
[34] J. Cui, Q. Cui, Q. Zhang, S. Li, An efficient multigram synthesis of juglone methyl ether, J. Chem. Res. 39 (2015) 553–554.
[35] Q. Zhang, J. Dong, Q. Cui, S. Li, J. Cui, Synthesis of 4,8-dimethoxy-1-naphthol via an acetyl migration, Synth. Commun. 47 (2017) 536–540.
[36] J. Cui, Q. Meng, X. Zhang, Q. Cui, W. Zhou, S. Li, Design and synthesis of new α-naphthoflavones as cytochrome P450 (CYP) 1B1 inhibitors to overcome docetaxel-resistance associated with CYP1B1 overexpression, J. Med. Chem. 58 (2015) 3534–3547.
[37] J. Cui, S. Li, J. Jia, A regioselective synthesis of 7-methyl juglone and its derivatives, Nat. Prod. Res. (2020), https://doi.org/10.1080/14786419.14782020.11761356.
[38] H. Möhrle, H. Folttmann, Eine neue plumbagin-synthese, Arch. Pharm. 321 (1988) 167–170.
[39] D.E. Zembower, C.M. Kam, J.C. Powers, L.H. Zalkow, Novel anthraquinone inhibitors of human leukocyte elastase and cathepsin G,, J. Med. Chem. 35 (1992) 1597–1605.
[40] J.L. Bloomer, K.W. Stagliano, J.A. Gazzillo, Preparation of functionalized juglone acetates and juglones via 1,4-dimethoxynaphthalene derivatives: synthesis of anthraquinones related to rhein and aloe-emodin, J. Org. Chem. 58 (1993) 7906–7912.
[41] C. Ye, P. Bian, J. Zhang, H. Xiao, L. Zhang, W. Ye, Y. Dong, Y. Zhou, Z. Jia, Y. Lei, Structure-based discovery of antiviral inhibitors targeting the E dimer interface of Japanese encephalitis virus, Biochem. Biophys. Res. Commun. 515 (2019) 366–371.
[42] M. Strugstad, S. Despotovski, A summary of extraction, properties, and potential uses of juglone: a literature review, J. Ecosyst. Manage. 13 (2012) 1–16.
[43] B.K. Aithal, M.R.S. Kumar, B.N. Rao, N. Udupa, B.S.S. Rao, Juglone, a naphthoquinone from walnut, exerts cytotoxic and genotoxic effects against cultured melanoma tumor cells, Cell Biol. Int. 33 (2009) 1039–1049.
[44] G.P. Husson, R. Vilagines, P. Delaveau, Recherche de proprietes antivirales de quelques extraits d' origine naturelle [Geranium robertsianum, Morus alba, Adianthum capillus veneris, Scrophularia aquatica, Juglans regia, Rauwolfia serpentina, Equisetum arvense, Ranunculus repens, Ailanthus glandulosa, Polypodium aureum, Polypodium vulgare, Dryopteris filix max], Ann. Pharm. Fr. 44 (1986) 41–48.
[45] H.C. Yang, S. Xing, L. Shan, K. O'Connell, J. Dinoso, A. Shen, Y. Zhou, C.K. Shrum, Y. Han, J.O. Liu, H. Zhang, J.B. Margolick, R.F. Siliciano, R.F. Siliciano, Small-molecule screening using a human primary cell model of HIV latency identifies compounds that reverse latency without cellular activation, J. Clin. Invest. 119 (2009) 3473–3486.
[46] C.-P. Chuck, H.-F. Chow, D.C.-C. Wan, K.-B. Wong, Profiling of substrate specificities of 3C-like proteases from group 1, 2a, 2b, and 3 coronaviruses, PloS One 6 (2011), e27228.
[47] S.A. Cherrak, H. Merzouk, N. Mokhtari-Soulimane, Potential bioactive glycosylated flavonoids as SARS-CoV-2 main protease inhibitors: a molecular docking and simulation studies, PloS One 15 (2020), e0240653.
[48] S.K. Enmozhi, K. Raja, I. Sebastine, J. Joseph, Andrographolide as a potential inhibitor of SARS-CoV-2 main protease: an in silico approach, J. Biomol. Struct. Dyn. (2020) 1–7.
[49] S. Garg, A. Roy, In silico analysis of selected alkaloids against main protease (Mpro) of SARS-CoV-2, Chem. Biol. Interact. 332 (2020) 109309.
[50] C. Muñoz-Fontela, W.E. Dowling, S.G.P. Funnell, P.-S. Gsell, A.X. Riveros-Balta, R.A. Albrecht, H. Andersen, R.S. Baric, M.W. Carroll, M. Cavaleri, C. Qin, I. Crozier, K. Dallmeier, L. de Waal, E. de Wit, L. Delang, E. Dohm, W.P. Duprex, D. Falzarano, C.L. Finch, M.B. Frieman, B.S. Graham, L.E. Gralinski, K. Guilfoyle, B.L. Haagmans, G.A. Hamilton, A.L. Hartman, S. Herfst, S.J.F. Kaptein, W.B. Klimstra, I. Knezevic, P.R. Krause, J.H. Kuhn, R. Le Grand, M.G. Lewis, W.-C. Liu, P. Maisonnasse, A.K. McElroy, V. Munster, N. Oreshkova, A.L. Rasmussen, J. Rocha-Pereira, B. Rockx, E. Rodríguez, T.F. Rogers, F.J. Salguero, M. Schotsaert, K.J. Stittelaar, H.J. Thibaut, C.-T. Tseng, J. Vergara-Alert, M. Beer, T. Brasel, J.F.W. Chan, A. García-Sastre, J. Neyts, S. Perlman, D.S. Reed, J.A. Richt, C.J. Roy, J. Segalés, S.S. Vasan, A.M. Henao-Restrepo, D.H. Barouch, Animal models for COVID-19, Nature 586 (2020) 509–515.
[51] K. Takayama, In vitro and animal models for SARS-CoV-2 research, Trends Pharmacol. Sci. 41 (2020) 513–517.
[52] B.N. Williamson, F. Feldmann, B. Schwarz, K. Meade-White, D.P. Porter, J. Schulz, N. van Doremalen, I. Leighton, C.K. Yinda, L. Pérez-Pérez, A. Okumura, J. Lovaglio, P.W. Hanley, G. Saturday, C.M. Bosio, S. Anzick, K. Barbian, T. Cihlar, C. Martens, D.P. Scott, V.J. Munster, E. de Wit, Clinical benefit of remdesivir in rhesus macaques infected with SARS-CoV-2, Nature 585 (2020) 273–276.